AgriEngineering

Article

Design and Performance Evaluation of an Integrated Sweet Potato Haulm Shredding and Harvesting Machine

Lu Zhu [1,2], Lin He [1,2], Kaihua Liu [1,2,*], Xiaodong Guan [1,2], Shi Xiong [1,2], Yong Gao [1,2], Wei Liu [1,2] and Minglin Chen [1,2]

[1] Guangdong Institute of Modern Agricultural Equipment, Guangzhou 510630, China; zhulu365@126.com (L.Z.); helin_gz@163.com (L.H.); 13359848935@163.com (X.G.); xiongs565@126.com (S.X.); andygao2024@163.com (Y.G.); 19854815556@163.com (W.L.); minglin.chen@163.com (M.C.)
[2] Key Laboratory of Modern Agricultural Intelligent Equipment in South China, Ministry of Agriculture and Rural Affairs of the People's Republic of China, Guangzhou 510630, China
* Correspondence: liukaihua96@163.com; Tel.: +86-137-1757-9795

Abstract

To address the inefficiencies of two-stage sweet potato harvesting in southern China, an integrated machine for synchronous haulm shredding and tuber excavation was developed. The equipment features a front-mounted, reverse-rotating crushing knife roller and a rear-mounted, adjustable grate-type digging shovel. The performance of the prototype was systematically evaluated through two-stage field trials in clay loam soil. First, an orthogonal test was employed to assess the haulm shredding quality. The results indicated that the knife roller speed significantly increased the qualified rate of crushed stems and leaves, whereas the forward speed exerted a negative effect. Additionally, the blade-to-ridge clearance primarily dictated the ridge-top stubble length. Second, a quadratic orthogonal rotational composite design was utilized to optimize the integrated harvesting parameters. The analysis demonstrated that shovel inclination significantly enhanced the tuber exposure rate, while both clearance and inclination exhibited quadratic nonlinear effects on the tuber damage rate. Multi-objective optimization established the optimal operational parameters as a blade-to-ridge clearance of 66.6 mm and a shovel inclination of 34.0°. Field validations under these settings achieved a tuber exposure rate of 83.7% and a damage rate of 4.3%, confirming the high reliability of the predictive models. The integrated equipment effectively shortens the harvesting cycle and demonstrates robust adaptability to clayey moist soils, thereby advancing the mechanization of sweet potato production.

Keywords: sweet potato harvesting; pre-harvest haulm shredding; hilly terrain; response surface methodology; multi-objective parameter optimization

Check for updates

Academic Editors: Jay Sul, Ramadas Narayanan and Tieneke Trotter

Received: 31 July 2026
Revised: 2 September 2026
Accepted: 4 September 2026
Published: 11 September 2026

Copyright: © 2026 by the authors. Licensee MDPI, Basel, Switzerland. This article is an open access article distributed under the terms and conditions of the Creative Commons Attribution (CC BY) license.

1. Introduction

Sweet potato is a vital root tuber crop grown across the globe, valued simultaneously as a staple grain and a commercial cash crop. Sweet potato plays an indispensable role in global agricultural systems, underpinning global food security, feed processing industries, and biomass energy development [1]. FAO 2021 statistics indicate that China is the world's leading sweet potato producer. The country boasts a planting area of 2.2061 million hm^2 (29.78% of the global cultivated area) and accounts for 53.83% of total global sweet potato yield [2]. Consequently, sweet potato constitutes one of the core crops for securing domestic food supplies and stimulating agricultural economic growth in China's extensive hilly and mountainous zones.

Sweet potato production is inherently labor-intensive. Pre-harvest haulm shredding pretreatment and tuber harvesting consume more than 60% of the total labor required throughout the whole production process, which represents the primary breakthrough target for realizing full mechanization [3–5]. Manual cutting of sweet potato vines is presented in Figure 1, and manual in-field collection of sweet potato tubers is shown in Figure 2.



Figure 1. Manual cutting of sweet potato vines.



Figure 2. Manual collection of sweet potatoes in the field.

Sweet potato vines grow prostrately on ridge surfaces and form a densely interwoven canopy, with individual vine lengths varying between 1.5 m and 4 m; the maximum vine biomass per unit area can reach 19.5 t/hm^2 [6]. If vines are not effectively shredded before tuber excavation, the dense vine canopy covering ridge surfaces will entangle the digging components and obstruct the operator's field of view, resulting in complete failure of harvesting operations [7–10].

Sweet potato cultivation in China still commonly adopts a two-stage operation system consisting of pre-harvest haulm shredding followed by tuber excavation. Such an operation mode is characterized by a prolonged working cycle and frequent machinery ingress into farmland. Moreover, the rainy autumn climate in southern China tends to delay the optimal harvesting period, which often delays the optimal harvest window and causes economic losses due to tuber rot and quality deterioration.

Scholars have carried out extensive research on structural optimization and performance improvement of pre-harvest haulm shredding equipment. Yang et al. designed a dual-shaft sweet potato vine beating and returning machine. The front vine picking device lifts the creeping vines on the ridge surface and throws them to the high-speed crushing knife roller, which strengthens the crushing effect of long vines and reduces the risk of knife roller entanglement and blockage [11,12]. Huang et al. developed a potato vine killer based on the negative pressure adsorption principle. The negative pressure field formed by the high-speed rotation of flail knives in the cavity adsorbs vine stems and

weeds, which improves the pre-harvest haulm shredding qualified rate while reducing accidental injury to underground tubers [13]. However, most pre-harvest haulm shredding machines are independent operation machines which cannot be operated synchronously with the subsequent excavation and harvesting process, making it difficult to meet the demand for rush harvesting.

In the field of sweet potato harvesting equipment, numerous studies have focused on the optimization of excavating components and the mechanism of tuber–soil separation. Conventional sweet potato harvesters lift the tuber–soil mixture through a digging shovel and screen soil during the lifting process through grate bars or conveyor chains; finally, the tubers fall onto the ridge surface to complete harvesting. Cai et al. developed a composite operation machine for sweet potato harvesting and vine recovery. The front disc cutter cuts the root of the vines, and the clamping and conveying mechanism transfers the vines to the vine collection box. Simultaneously, the digging shovel and vibrating separation conveyor complete the tuber harvesting, realizing multi-process integrated operation [14], but it has a complex structure, large overall size and mass, and is more suitable for plain large-scale planting plots, making it difficult to operate in scattered small fields in hilly and mountainous areas of southern China [15–17].

To address the above industrial pain points and research gaps, this study proposes a compact single-pass integrated sweet potato haulm shredding and harvesting machine specifically adapted to small, scattered fields in hilly regions of southern China. The main novelties and contributions are as follows: (1) structural innovation: a front-mounted counter-rotating knife roller with staggered ridge-profiled blades is adopted to achieve full-coverage shredding of ridge surfaces and furrows without an additional vine-lifting device, effectively reducing machine size and complexity. (2) Integrated configuration: the machine combines haulm shredding and grate-type tuber excavation in a single three-point hitch-mounted unit, with overall dimensions of only 1245 × 1430 × 1000 mm, making it compatible with small and medium tractors and suitable for hilly terrains. (3) Systematic performance quantification: two-stage field experiments (orthogonal test + response surface optimization) are conducted under typical clay loam conditions in southern China, revealing the multi-parameter coupling mechanism and obtaining optimized operational parameters. The research results can provide a theoretical basis and technical reference for the optimal design and popularization of compact integrated sweet potato harvesting equipment in hilly and mountainous areas.

2. Materials and Methods

2.1. Machine Structure

Figure 3 illustrates the structural configuration of the integrated pre-harvest haulm shredding and tuber excavation machine for sweet potatoes. The implement is assembled from multiple functional components, including the haulm crushing unit, chain casings, transmission assembly, half-shaft sleeves, adjustment screws, drive shafts, connecting brackets, land wheels, vine lifting cutters and digging shovels. The machine features overall dimensions of 1245 × 1430 × 1000 mm and is capable of performing pre-harvest vine shredding and tuber harvesting simultaneously in one field operation. Attached to the tractor through a standard three-point hitch mounted on the front frame, the machine is propelled forward by the tractor during field work. As shown in Figure 4, power for the haulm crushing system is supplied by the tractor. The tractor power take-off (PTO) is connected to the input shaft of the integrated machine via a transmission shaft. A two-stage speed increase is achieved via a gearbox and sprocket drive, enabling the shredding knife rotor to rotate at 2000–3000 r/min. Such rotational speed endows the cutting blades with sufficient peripheral linear speed to achieve effective haulm shredding.

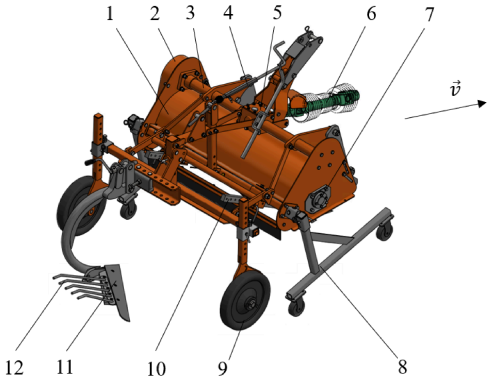

Figure 3. Structure of the integrated sweet potato pre-harvest haulm shredding and excavating machine. 1. Crushing system outer shell; 2. chain cover; 3. transmission system half-shaft sleeve; 4. adjusting screw; 5. cross reversing gearbox; 6. transmission shaft; 7. bearing mounting seat; 8. transfer bracket; 9. ground wheel; 10. vine picking knife; 11 and 12. digging shovel.

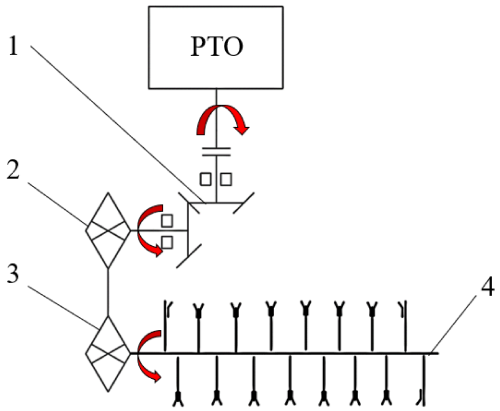

Figure 4. Power transmission route. 1. Cross reversing gearbox; 2. driving sprocket; 3. driven sprocket; 4. crushing knife roller.

The structural installation diagram of the crushing device is shown in Figure 5. The device is mainly composed of knife roller, straight blades, L-shaped blades, small bent blades, long blades, bearing end covers, bearing seats, bearings, oil seals and other components.

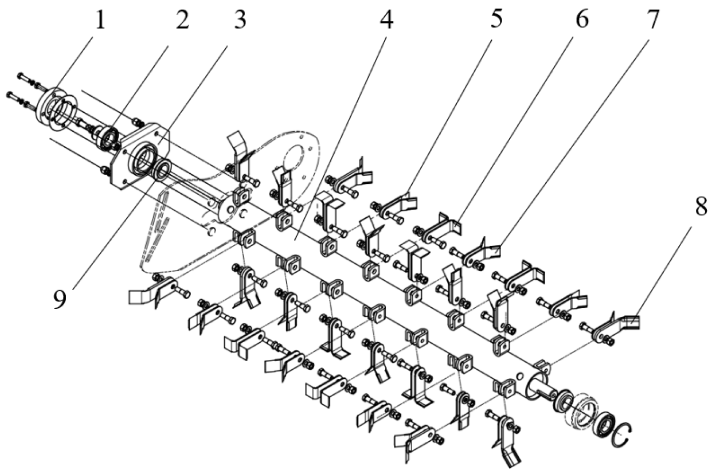

Figure 5. Structural installation diagram of the crushing device. 1. Bearing end cover; 2. bearing; 3. bearing seat; 4. knife roller; 5. straight blade; 6. L-shaped blade; 7. small bent blade; 8. long blade; 9. oil seal.

According to relevant research, the reverse design of the knife roller shaft, so that it forms a trochoid motion trajectory, can prevent vine pushing during machine operation. Therefore, the knife roller shaft is also designed to rotate reversely in this paper. The motion trajectory of the flail blade tip is analyzed. Taking the axis center of the knife roller shaft as the coordinate origin, the forward direction of the machine as the positive direction of the x-axis, and the vertical downward direction as the positive direction of the y-axis, the motion trajectory of the flail blade tip is:

$$\begin{cases} x = vt - Rcos\omega t \\ y = Rsin\omega t \end{cases} \quad (1)$$

where:

v—forward speed of the machine, taken as 1 m/s in this paper;

R—radius of gyration of the flail blade tip, taken as 0.17 m in this paper;

ω—angular velocity of knife roller rotation, rad/s.

By derivation, the instantaneous velocity of the flail blade tip is:

$$\begin{cases} v_x = v + R\omega sin\omega t \\ v_y = R\omega cos\omega t \end{cases} \quad (2)$$

The quality of vine cutting operation is affected by the horizontal component velocity of the flail blade. To crush sweet potato vines well, the absolute value of the horizontal component velocity of the flail blade shall not be lower than the linear speed required for vine cutting, so that it has a sufficiently large forward component, i.e., $v_x \geq v_c$. Considering that the root of the blade edge also participates in vine cutting, v_x shall be calculated based on the root of the blade edge. Therefore, the calculation formula for the minimum speed of the knife roller is:

$$n \geq 30(v_c - v)/[\pi(R - h)] \quad (3)$$

where:

n—knife roller speed, r/min;

v_c—minimum linear speed required for clean vine cutting, 30 m/s. This value was derived from rotary cutting bench tests of sweet potato stems in previous studies [18,19], representing the threshold speed to avoid stem tearing and knife roller winding;

h—blade edge length, taken as 0.04 m in this paper.

Under stable working conditions, the forward speed of the machine is 1 m/s, the minimum linear speed required for vine cutting at the root of the blade edge v_c = 30 m/s, and the blade length h = 0.04 m. Substituting the above data into Formula (3), the calculated knife roller speed shall be no less than 2130 r/min. The rated speed of the knife roller is designed to be about 2200 r/min through the cross reversing gearbox and two-stage sprocket acceleration of the sweet potato vine killer.

Figure 6 demonstrates the structural layout of the sweet potato digging share. This component is composed of a mounting bracket, front connection base, steel pipe components, cutting blade, side mouldboard and grate bars. The design of the cutting blade complies with both agricultural machinery operation requirements and agronomic regulations, tailored to the growth rules and ridge planting mode of sweet potatoes. The blade width is determined by the spatial distribution characteristics of tubers. In the harvesting process, tubers are predominantly concentrated in the middle section of ridges, confined within the range of 300–350 mm. For this reason, the cutting blade width is set to 350 mm, which is structurally reasonable. The digging share is configured as a flat shovel structure,

with its stress schematic illustrated in Figure 7. The theoretical value of the horizontal dip angle α of the cutting blade can be solved using the force equilibrium Equation (4) for excavated soil presented in Figure 7.

$$\begin{cases} Pcos\alpha - F_f - Gsin\alpha = 0 \\ F_n - Gcos\alpha - Psin\alpha = 0 \\ F_f = \mu(Gcos\alpha + Psin\alpha) \end{cases} \quad (4)$$

where:

P—force required for the excavated material to move along the ground;
α—inclination angle between the digging shovel blade and the horizontal direction;
F_n—supporting force of the shovel surface on the soil;
G—gravity of the excavated material;
F_f—friction force of the shovel surface on the excavated material;
μ—friction coefficient between the shovel surface and the excavated material.

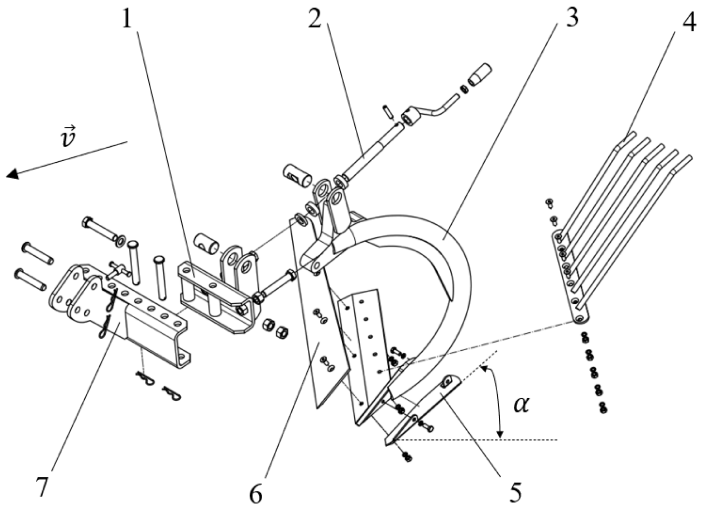

Figure 6. Installation diagram of the digging shovel. 1. Mounting frame; 2. lead screw; 3. main plow body; 4. grate bar; 5. side plow body; 6. digging shovel blade; 7. front mounting seat.

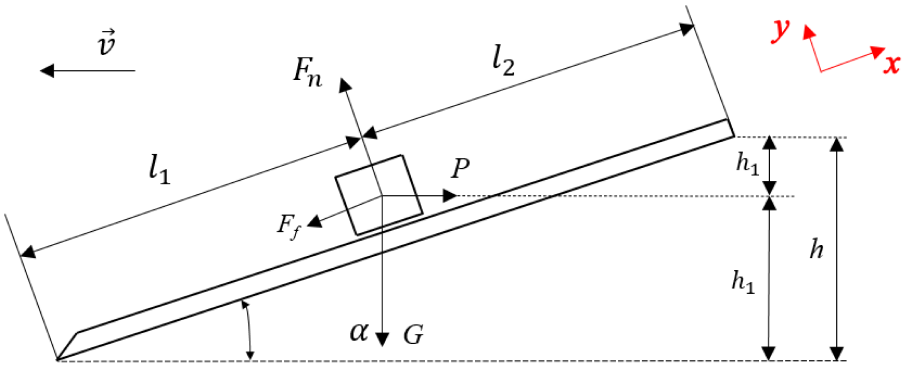

Figure 7. Force diagram of digging shovel blade on excavated material.

Increasing the inclination angle α is conducive to breaking soil clods and increasing the tuber exposure rate, but it will also increase the working resistance of the shovel [20]. Based on the force equilibrium model in Equation (4), with the soil–shovel friction coefficient μ taken as 0.45 (typical for clay loam in southern China) and the tuber–soil bulk density taken as 1.6 g/cm^3, the theoretical optimal inclination angle for low-resistance excavation is calculated to be approximately 22–28°. The force equilibrium model is valid for inclination angles in the range of approximately 10–40°; beyond 40°, soil dispersion and cohesion

loss would reduce the accuracy of the model. To adapt to variations in soil moisture, ridge height and tuber distribution depth under actual field conditions, and to ensure the validity of the mechanical model, the adjustment range of the digging shovel blade inclination angle α is designed to be 15–35°. The excavation inclination angle α can be adjusted through the lead screw. When the lead screw rotates clockwise, the digging shovel rotates counterclockwise about the lower mounting hole, thereby increasing the inclination angle α.

Note: l_1 is the front length of the digging shovel; l_2 is the rear length of the digging shovel; α is the inclination angle between the digging shovel blade and the horizontal direction; P is the force required for the excavated material to move along the shovel surface; F_n is the supporting force of the shovel surface on the soil; G is the gravity of the excavated material; F_f is the friction force of the shovel surface on the excavated material; $\vec{v}$ is the direction of the forward speed of the machine.

2.2. Field Test Conditions

To verify the actual operation effect of the integrated sweet potato pre-harvest haulm shredding and excavating machine, field tests were arranged to test the pre-harvest haulm shredding and excavation operation performance of the prototype. The test was conducted in October 2025 at Dapotian, Lanziwei Village, Lancheng Town, Dongyuan County, Heyuan City, Guangdong Province. The soil type of the test field is clay loam. Planting ridges are built wide to drain excess soil water and avoid waterlogging damage. During harvesting, the ridge height is 38 cm; the distance between adjacent ridges is 135 cm; the tested sweet potato cultivar was 'Pushu 32' (commercial name: Xiguahong), a red-fleshed variety widely grown in southern China; and the tuber setting depth is 200~300 mm [21]. Before the field experiment, the drip pipes on the ridges were manually removed, and no treatment was performed on the vines. The supporting power is a Lovol 804 tractor (Weichai Lovol Intelligent Agriculture Technology Co., Ltd., Weifang, China).

2.2.1. Evaluation Criteria for Operation Quality

The field experiment was formulated in strict accordance with three Chinese agricultural industry standards: NY/T 2706-2015 (Technical Specification for Quality Evaluation of Potato Haulm Toppers) [22], JB/T 14284-2022 (Potato Haulm Toppers) [23] and NY/T 4478-2025 (Technical Regulations for Sweet Potato Harvesting) [24], The main performance indicators measured include qualified rate of crushed stem–leaf length, stubble length, tuber exposure rate, tuber damage rate and other parameters.

All mass measurements were performed using a portable electronic scale with an accuracy of ± 0.01 kg. Length measurements (stubble length, tuber size) were performed using a steel tape with an accuracy of ± 1 mm. Each treatment was replicated at 5 sampling points along the test row, and each sampling point was measured 3 times to reduce random error. The overall experimental uncertainty was estimated as follows: the relative standard deviation (RSD) of the crushing qualified rate was 1.2–2.1%, the RSD of stubble length was 3.5–5.2%, and the RSD of tuber exposure rate and tuber damage rate was 2.3–3.8%. All measurement errors were within acceptable ranges for agricultural field experiments.

The length qualified rate of crushed stems and leaves is calculated using Equation (5). All crushed stems and leaves are collected and weighed at each sampling point, after which fragments with a length greater than 200 mm are sorted out and weighed separately. The final result is taken as the average value across 10 sampling points.

$$D_h = \frac{m_y - m_b}{m_y} \times 100 \quad (5)$$

where:

D_h is qualified rate of crushed stem–leaf length at each measuring point, %;

m_y is mass of crushed stems and leaves at each measuring point, kg;

m_b is mass of stems and leaves with crushed length greater than 200 mm at each measuring point, kg.

Stubble length is defined as the length of vine stems remaining uncut on the ridge top after the pre-harvest mechanical haulm shredding operation. Excessively long stubble impairs sweet potato excavation, whereas excessively short stubble means the blades cut closer to the ridge surface, which increases the risk of mechanical damage to shallow-growing tubers. A stubble length in the range of 50–100 mm is considered common. Stubble length is measured at 10 consecutive sampling points, and the final mean value is calculated according to Equation (6):

$$\overline{h} = \frac{\sum_{i=1}^{10} h_i}{10} \tag{6}$$

where:

$\overline{h}$ is average stubble length, mm;

h_i is residual vine stem length at the measuring point, mm.

For the determination of tuber exposure rate and tuber damage rate, all exposed tubers in the sampling area are collected first, and all buried unharvested tubers are manually excavated afterwards. All recovered tubers are sorted into damaged and undamaged groups and weighed separately. The tuber exposure rate and tuber damage rate are calculated using Equations (7) and (8), respectively:

$$T_0 = \frac{W_0}{W} \times 100 \tag{7}$$

$$T_S = \frac{W_S}{W} \times 100 \tag{8}$$

where:

T_0 is tuber exposure rate, %;

W_0 is mass of exposed tubers in the measurement area, kg;

W is total mass of sweet potatoes in the measurement area, kg;

T_S is tuber damage rate, %;

W_S is mass of damaged tubers in the measurement area, kg.

Measure 12 areas according to the above formulas, and calculate the average values of tuber exposure rate and tuber damage rate.

2.2.2. Test Scheme for Pre-Harvest Haulm Shredding Operation

To evaluate the pre-harvest haulm shredding performance of the integrated machine and eliminate interference from the excavating device on measurement accuracy, the digging shovel mounted at the rear of the machine was removed prior to each haulm shredding operation. The height of the depth-limiting wheel was calibrated before each test run.

Three key factors influencing haulm shredding effect were selected for the orthogonal test: machine forward speed (Factor A), blade-to-ridge clearance (Factor B), and knife roller rotational speed (Factor C). An L_9 (3^3) orthogonal array with three levels per factor was adopted for the experiment. The factor levels are listed in Table 1. All trials were carried out per the experimental design to investigate the influence of each factor on haulm shredding operation quality.

Table 1. Test factor level table.

Coding Level	Forward Speed A/(m/s)	Blade-to-Ridge Clearance B/(mm)	Knife Roller Speed C/(r/min)
−1	0.5	20	2100
0	1.5	50	2500
1	2.5	80	2900

2.2.3. Field Experiment Scheme for Integrated Pre-Harvest Haulm Shredding and Excavating Operation

To verify the operational performance of the front-end integrated pre-harvest haulm shredding and excavation unit and identify optimal operating parameters, field tests of the integrated operation were conducted after the completion of standalone pre-harvest haulm shredding trials.

The blade-to-ridge clearance of the prototype and the excavation inclination angle of the digging shovel are critical factors affecting both pre-harvest haulm shredding quality and sweet potato harvesting performance. To optimize these two parameters, a response surface experiment with a quadratic orthogonal rotational combination design was carried out under fixed operating conditions: a forward speed of 1.5 m/s and a knife roller speed of 2500 r/min.

These baseline values were selected as a practical engineering compromise: (1) a forward speed of 1.5 m/s is the typical operating speed of small and medium tractors in hilly fields of southern China, balancing work efficiency and operation stability; (2) a knife roller speed of 2500 r/min achieves a crushing qualified rate above 93% (verified in the orthogonal test), fully meeting industry quality requirements, while avoiding excessive power consumption and vibration caused by higher rotational speeds.

A dual-indicator mathematical model was constructed via multiple regression fitting. Combined with analysis of variance (ANOVA) and three-dimensional response surface plots, the influence law of the two-factor interaction on sweet potato harvesting performance was clarified.

Based on the test results of the integrated pre-harvest haulm shredding machine, an excessively small blade-to-ridge clearance increases the tuber damage rate, while an excessively large value increases the stubble length at the ridge top. Accordingly, the blade-to-ridge clearance was set within the range of 10–90 mm, and the digging shovel inclination angle was set within 15°~35°. The test factor levels are listed in Table 2.

Table 2. Test factor coding table.

Code	Blade-to-Ridge Clearance X_1 (mm)	Digging Shovel Inclination X_2 (°)
−1.414	10	15
−1	21.7	17.9
0	50	25
1	78.3	32.1
1.414	90	35

Note: −1.414 = axial point, 0 = central point, ±1 = factorial point for quadratic orthogonal rotational composite design.

2.3. Statistic

All experimental data were preprocessed and calculated in strict accordance with the test methods specified in NY/T 2706-2015, JB/T 14284-2022 and NY/T 4478-2025. Each treatment was set with repeated sampling measurements, and the results were expressed as mean values. All statistical analysis, model fitting and visualization were completed by Design-Expert 13 (Stat-Ease Inc., Minneapolis, MN, USA) and SPSS 26.0 (IBM Corp., Armonk, NY, USA). The significance level of statistical tests was set at $\alpha = 0.05$.

For the independent haulm shredding orthogonal experiment, range analysis was first performed to sort the influence weight of forward speed (A), blade-to-ridge clearance (B) and knife roller speed (C) on the qualified rate of stem–leaf crushing and average stubble length so as to preliminarily determine the primary and secondary order of influencing factors. On this basis, one-way analysis of variance (ANOVA) was carried out to test the statistical significance of each factor on the evaluation indexes. The significance levels were defined as follows: *** represents highly significant difference ($p < 0.01$), ** represents significant difference ($0.01 \leq p < 0.05$), and * represents relatively significant difference ($0.05 \leq p < 0.1$). The optimal parameter combination for independent haulm shredding operation was determined by combining range analysis and variance analysis results.

For the integrated haulm shredding and excavating experiment, a quadratic regression orthogonal rotary combination design was adopted to construct the quantitative mapping relationship between operating parameters and harvesting performance. Taking blade-to-ridge clearance (X_1) and digging shovel inclination (X_2) as independent variables, and tuber exposure rate (Y_1) and tuber damage rate (Y_2) as response values, multivariate regression fitting was carried out to establish a second-order polynomial regression model for each response index. To improve the accuracy of prediction results, the coefficients of the regression equation are rounded to four decimal places. ANOVA was performed on the optimized regression model to verify the overall significance of the model and the significance of each term coefficient, and the lack-of-fit test was used to evaluate the fitting degree and reliability of the model. Three-dimensional response surface plots were drawn to intuitively reveal the coupling effect of dual factors on each harvest index.

Finally, multi-objective parameter optimization was carried out with the goals of maximizing the tuber exposure rate and minimizing the tuber damage rate, and the global optimal operating parameter combination was solved. To verify the prediction accuracy of the regression model and the field feasibility of the optimal parameters, five repeated field validation tests were carried out under the optimal parameter conditions. The relative error between the measured average value and the model predicted value was calculated to confirm the reliability and engineering applicability of the optimization results.

3. Results

3.1. Analysis of Independent Pre-Harvest Haulm Shredding Orthogonal Test Results

3.1.1. Analysis of Qualified Rate of Crushed Stem–Leaf Length Index

Range analysis showed that the influence weight of the three factors on the crushing qualified rate followed the order: knife roller speed (C) > forward speed (A) > blade-to-ridge clearance (B).

The range value for knife roller speed (C) was 4.87 compared with 1.66 for forward speed (A) and only 0.30 for blade-to-ridge clearance (B). This result indicates that knife roller speed is the dominant parameter determining haulm shredding quality, forward speed serves as a secondary regulatory factor, and blade-to-ridge clearance exerts no notable effect on crushing qualification performance.

Analysis of variance (ANOVA) results demonstrated that knife roller speed (C) had an F-value of 418.23 ($p < 0.01$), exerting a highly significant effect on the length qualified rate of crushed stems and leaves. Forward speed (A) yielded an F-value of 51.77 ($0.01 < p < 0.05$), indicating a significant effect on the qualified rate. Blade-to-ridge clearance (B) had an F-value of 1.62 ($p > 0.05$), showing no statistically significant influence (see Tables 3 and 4).

This variation pattern can be explained from the perspective of haulm shredding dynamics. Increasing the knife roller speed directly elevates the effective cutting linear velocity of the blades, enhances the shearing and crushing effect on long vines and thick stems, and thus substantially reduces the proportion of overlong residual vines. This trend

also verifies that the 30 m/s cutting speed threshold adopted in the theoretical design is reasonable and applicable under field conditions. As forward speed increases, the mass of vines fed to the knife roller per unit time increases, and the number of cutting impacts per unit length of vine decreases, reducing the crushing qualified rate. This easily results in incompletely crushed long vines, leading to a slight decline in the crushing qualified rate. Blade-to-ridge clearance only adjusts the vertical distance between the flail blades and the ridge surface, which merely changes the reference cutting height without altering the relative cutting speed between the blades and vines. Accordingly, it has no significant regulatory effect on haulm shredding particle size.

Table 3. Orthogonal test results of pre-harvest haulm shredding operation.

No.		Forward Speed *A* (m/s)	Blade-to-Ridge Clearance *B* (mm)	Knife Roller Speed *C* (r/min)	Crushing Qualified Rate (%)	Stubble Length (mm)
1		0.5	20	2100	89.9	41
2		0.5	50	2500	94.4	56
3		0.5	80	2900	92.4	97
4		1.5	20	2500	93.3	39
5		1.5	50	2900	91.5	55
6		1.5	80	2100	88.2	99
7		2.5	20	2900	91.1	37
8		2.5	50	2100	87.8	59
9		2.5	80	2500	92.8	97
Crushing qualified rate	t1	92.23	91.43	88.63		
	t2	91	91.23	93.5	Ranking of influencing factors: C > A > B	
	t3	90.57	91.13	91.67	Optimal combination: $A_1B_2C_2$	
Stubble length	t1	64.67	39	66.33		
	t2	64.33	56.67	64	Ranking of influencing factors: B > C > A	
	t3	64.33	97.67	63	Optimal combination: $A_3B_1C_3$	

Table 4. ANOVA of orthogonal test.

Evaluation Index	Error Source	Sum of Squares	df	Mean Square	F-Value	Significance
Crushing qualified rate	*A*	4.49	2	2.24	51.77	**
	B	0.14	2	0.07	1.62	
	C	36.25	2	18.12	418.23	***
	Error	0.09	2	0.04		
	Total	40.96	8			
Stubble length	*A*	0.22	2	0.11	0.14	
	B	5434.89	2	2717.44	3493.86	***
	C	17.56	2	8.78	11.29	*
	Error	1.56	2	0.78		
	Total	5454.22	8			

Note: *** means highly significant ($p < 0.01$); ** means significant ($0.01 < p < 0.05$); * means relatively significant ($0.05 < p < 0.1$).

According to the mean values of each factor level, the optimal parameter combination for the crushing length qualified rate was $A_1B_2C_2$, corresponding to a forward speed of 0.5 m/s, a blade-to-ridge clearance of 50 mm, and a knife roller speed of 2500 r/min. Under this experimental condition, the machine operates at low forward speed with a medium-high knife roller speed, ensuring that vines per unit length receive sufficient impacts and cutting passes. In the orthogonal test, the crushing qualified rate under this condition reached 94.4%, which fully satisfies the industry quality standard requiring crushed vine length $\leq$ 200 mm for sweet potato pre-harvest haulm shredding and field returning.

3.1.2. Analysis of Average Ridge-Top Stubble Length Index

Taking the average length of residual vine stems on the ridge top as the evaluation index, range analysis of the orthogonal test revealed that the three factors ranked in the following order of influence: blade-to-ridge clearance (*B*) > knife roller speed (*C*) > forward speed (*A*). The range value for blade-to-ridge clearance reached 58.67, compared with 3.33 for knife roller speed and less than 0.34 for forward speed, indicating that blade-to-ridge clearance is the dominant factor governing stubble height.

Analysis of variance (ANOVA) further confirmed the significance of these effects. Blade-to-ridge clearance (*B*) yielded an F-value of 3493.86 ($p < 0.01$), exerting a highly significant effect on stubble length. Knife roller speed (*C*) had an F-value of 11.29 ($0.05 < p < 0.1$), indicating a marginally significant effect. Forward speed (*A*) returned an F-value of 0.14 ($p > 0.05$) and showed no statistically significant influence.

This pattern can be explained by the agronomic-structural matching mechanism of the machine. Blade-to-ridge clearance directly determines the vertical distance between the lower edge of the flail blades and the ridge surface. A smaller clearance lowers the reference cutting height of the blades, resulting in a lower cutting position at the base of sweet potato vines and a corresponding reduction in residual stem length on the ridge top. With excessive clearance, the blades only cut the middle and upper sections of the vines, leaving large amounts of vine bases intact on the ridge surface and thus markedly increasing stubble length.

Knife roller speed exerts only a weak auxiliary regulatory effect: increasing rotational speed delivers repeated impacts on a small portion of lodged, ground-hugging short vines, slightly reducing residual stubble length. Forward speed merely alters the horizontal feed rate of the machine, without changing the vertical cutting height of the blades, and therefore has negligible effect on stubble length regulation.

In accordance with the agronomic requirements for sweet potato harvesting (reasonable stubble range: 50–100 mm), the optimal parameter combination for stubble length was $A_3B_1C_3$, corresponding to a forward speed of 2.5 m/s, a blade-to-ridge clearance of 20 mm, and a knife roller speed of 2900 r/min. Under this condition, the blades cut close to the ridge surface, yielding an average stubble length of only 37 mm, which prevents long stubble from entangling the subsequent digging shovel.

However, this parameter set presents an inherent trade-off: at high forward speed and small blade-to-ridge clearance, even with high knife roller speed, the haulm shredding qualified rate only reaches 91.1%, with a drawback that the crushed vine particle rate is 91.1%, just slightly exceeding 90%. Therefore, practical integrated operation must balance crushing qualified rate and stubble height, adopting a compromised parameter range to match the operational requirements of the entire machine.

The optimal parameter combinations for the two evaluation indices cannot be fully aligned, reflecting a parameter coupling contradiction between crushing qualified rate and low stubble height in pre-harvest haulm shredding operations. A low blade-to-ridge clearance shortens stubble but does not improve haulm shredding performance; high knife roller speed combined with low forward speed optimizes the haulm shredding effect but cannot reduce residual stubble height on the ridge surface.

For actual field operation, parameters should be selected with compromise under the constraint of integrated harvesting indices so as to provide parameter boundary references for subsequent response surface optimization of the combined pre-harvest haulm shredding and excavation operation.

3.2. Results of the Field Experiment of Integrated Pre-Harvest Haulm Shredding and Excavation Operation Based on Quadratic Orthogonal Rotational Composite Design

A response surface experiment with a quadratic orthogonal rotational composite design was conducted to evaluate sweet potato harvesting performance. Tests were carried out under baseline conditions: a fixed forward speed of 1.5 m/s and a rated knife roller speed of 2500 r/min. Blade-to-ridge clearance (X_1) and digging shovel inclination angle (X_2) were selected as test factors, while tuber exposure rate (Y_1) and tuber damage rate (Y_2) were adopted as dual response indicators for harvesting quality. A dual-indicator mathematical model was established via multiple regression fitting, and the interaction effects of the two factors on harvesting performance were analyzed through analysis of variance (ANOVA) and three-dimensional response surface plots.

The field integrated operation of pre-harvest haulm shredding and excavation is illustrated in Figures 8 and 9. The test results are summarized in Table 5, and the significance test results of the regression equations are presented in Table 6. Both regression models for tuber exposure rate (Y_1) and tuber damage rate (Y_2) are highly significant ($p < 0.01$), indicating good fitting performance. Blade-to-ridge clearance (X_1) has no significant effect on tuber exposure rate (Y_1), whereas digging shovel inclination angle (X_2) exerts a highly significant effect on Y_1.

Table 5. Integrated pre-harvest haulm shredding and excavating operation test.

No.	Blade-to-Ridge Clearance X_1 (mm)	Digging Shovel Inclination X_2 (°)	Tuber Exposure Rate Y_1 (%)	Tuber Damage Rate Y_2 (%)
1	21.7	17.9	82.2	4.9
2	78.3	17.9	82.0	3.8
3	21.7	32.1	84.1	5.2
4	78.3	32.1	83.8	4.1
5	10	25	83.2	5.7
6	90	25	82.8	2.8
7	50	15	81.5	3.8
8	50	35	84.2	5.1
9	50	25	83.1	3.5
10	50	25	83.0	3.4
11	50	25	83.9	3.5
12	50	25	83.1	3.6
13	50	25	83.2	3.7



Figure 8. Sweet potato pre-harvest haulm shredding operation test in progress.

For tuber damage rate (Y_2), both blade-to-ridge clearance (X_1) and the quadratic term of digging shovel inclination angle ($X_2{}^2$) show significant effects, while both digging shovel inclination angle (X_2) and the quadratic term of blade-to-ridge clearance ($X_1{}^2$) exert highly significant effects.



Figure 9. Effect diagram of sweet potato pre-harvest haulm shredding operation.

Table 6. ANOVA of regression equations.

Source		Sum of Squares	df	Mean Square	F-Value	*p*-Value	Significance
Tuber exposure rate	Model	7.48	5	1.5	18.9	0.0006	***
	X_1	0.142	1	0.142	1.79	0.2224	
	X_2	7.07	1	7.07	89.23	<0.0001	***
	X_1X_2	0.0025	1	0.0025	0.0316	0.864	
	X_1^2	0.0767	1	0.0767	0.9686	0.3578	
	X_2^2	0.2254	1	0.2254	2.85	0.1354	
	Residual	0.5543	7	0.0792			
	Lack of fit	0.0223	3	0.0074	0.0559	0.9803	
	Pure error	0.532	4	0.133			
	Total	8.04	12	1.5			
Tuber damage rate	Model	8.32	5	1.66	20.16	0.0005	***
	X_1	0.7182	1	0.7182	8.70	0.0214	**
	X_2	5.78	1	5.78	70.06	<0.0001	***
	X_1X_2	0.0625	1	0.0625	0.7573	0.413	
	X_1^2	1.06	1	1.06	12.82	0.009	***
	X_2^2	0.9268	1	0.9268	11.23	0.0122	**
	Residual	0.5777	7	0.0825			
	Lack of fit	0.4497	3	0.1499	4.68	0.0849	
	Pure error	0.128	4	0.032			
	Total	8.9	12	1.66			

Note: *** means highly significant ($p < 0.01$); ** means significant ($0.01 < p < 0.05$).

Multiple regression fitting of the experimental data was performed using Design-Expert 13 software. To enhance prediction precision, regression coefficients are retained to four decimal places. Consequently, model terms with absolute coefficients less than 0.0001 are considered negligible and have been omitted. The regression equations for the tuber exposure rate (Y_1) and tuber damage rate (Y_2) were obtained as follows:

$$Y_1 = 77.4712 - 0.0115X_1 + 0.3171X_2 - 0.0036X_2^2 \quad (9)$$

$$Y_2 = 12.1080 - 0.0437X_1 - 0.4507X_2 + 0.0005X_1^2 + 0.0072X_2^2 \quad (10)$$

3.2.1. Analysis of Variance Significance Test of Regression Model

Quadratic polynomial regression fitting was conducted on 13 sets of experimental data using Design-Expert 13 software, and separate regression prediction models were developed for the tuber exposure rate and tuber damage rate. The analysis of variance (ANOVA) results for the two models are summarized in Table 6.

(1) Tuber exposure rate model ($Y_1 = 77.4712 - 0.0115X_1 + 0.3171X_2 - 0.0036X_2^2$)

The overall model was highly significant ($p = 0.0006 < 0.01$), and the lack-of-fit term was not statistically significant ($p = 0.9803 > 0.05$). This indicates that the regression equation has satisfactory fitting accuracy, with no omitted significant terms, and is suitable for parameter prediction and optimization.

For individual model terms: the linear term of digging shovel inclination angle (X_2) exerted a highly significant positive effect on the tuber exposure rate ($p < 0.0001$). The linear term of blade-to-ridge clearance (X_1), the interaction term X_1X_2, and the quadratic terms ${X_1}^2$ and ${X_2}^2$ all showed no statistically significant effects (all $p > 0.05$).

(2) Tuber damage rate model ($Y_2 = 12.108 - 0.0437X_1 - 0.4507X_2 + 0.0005X_1^2 + 0.0072X_2^2$)

The overall model was highly significant ($p = 0.0005 < 0.01$), with a non-significant lack-of-fit term ($p = 0.0849 > 0.05$), confirming good reliability of the model.

Significance analysis of each term revealed that the linear term of digging shovel inclination angle (X_2) was highly significant ($p < 0.0001$), the linear term of blade-to-ridge clearance (X_1) was significant ($p = 0.0214$), the quadratic term of blade-to-ridge clearance (${X_1}^2$) was highly significant ($p = 0.009$), and the quadratic term of digging shovel inclination angle (${X_2}^2$) was significant ($p = 0.0122$). The two-factor interaction term X_1X_2 yielded a p-value of 0.413 ($p > 0.05$), indicating an insignificant interaction effect.

3.2.2. Analysis of Single-Factor Action Law

(1) Digging shovel inclination X_2

Digging shovel inclination angle is the core factor governing both the tuber exposure rate and tuber damage rate, exerting highly significant effects on both indicators.

The tuber exposure rate exhibits a monotonically linear increasing trend with rising digging shovel inclination angle. Increasing the shovel inclination lifts the tuber–soil mixture to a greater height, extends the conveying distance along the grate bars, and provides longer time for soil separation, thus improving the tuber exposure rate. This allows soil to fall sufficiently through the gaps between grate bars and exposes tubers on the ridge surface, thereby increasing the tuber exposure rate synchronously. At an excessively small inclination angle (approximately 15°), the gentle shovel surface provided insufficient lifting height for the tuber–soil mixture, leaving a large number of tubers embedded in the soil within the ridge body; the tuber exposure rate was only 81.5% under this condition.

The tuber damage rate follows a quadratic trend of initial decrease followed by subsequent increase with growing inclination angle. At low inclination angles, the gentle shovel surface results in low sliding friction magnitude on tubers, but insufficient tuber–soil separation leads to latent damage in tubers caused by soil clod extrusion. With a moderate increase in inclination angle (25–32°), the tuber–soil separation effect reaches its optimum; the probability of rigid impacts between tubers, hard soil clods and the shovel blade is greatly reduced, and the tuber damage rate drops to its minimum value. When the inclination angle exceeds 32.1°, the steep shovel surface causes tubers to roll down rapidly and collide with the grate bars, exacerbating mechanical impact damage and leading to a rebound in the tuber damage rate.

(2) Blade-to-ridge clearance X_1

Blade-to-ridge clearance (X_1) primarily regulates the reference cutting height of pre-harvest haulm shredding, indirectly influences the risk of tuber damage, and exerts no significant effect on the tuber exposure rate.

When the clearance varies within 10–90 mm, the tuber exposure rate only fluctuates marginally without a distinct increasing trend. Since blade-to-ridge clearance only affects the haulm shredding process on the ridge surface and does not alter the soil penetration

behavior of the digging shovel or the tuber–soil separation structure, it has no regulatory effect on tuber exposure performance.

The tuber damage rate follows an upward-opening parabolic trend with increasing blade-to-ridge clearance. At excessively small clearances (10–20 mm), the lower edge of the flail blades lies close to the ridge surface, and high-speed rotating blades are prone to scratch and incise shallow-growing tubers, leading to a marked rise in the proportion of skin breakage and cutting damage.

As the clearance gradually increases to approximately 43.7 mm, the blades move away from the tuber growth layer, completely eliminating the risk of blade impact on tubers and causing the tuber damage rate to decrease continuously. When the clearance exceeds 43.7 mm, overlong ridge-top stubble and residual thick stems become entangled with the digging shovel blade. Tubers are twisted and compressed along with the entangled vines, resulting in a slight rebound in the tuber damage rate.

3.2.3. Response Surface Analysis of Factor Interaction Effects

The response surfaces for the interaction between blade-to-ridge clearance (X_1) and digging shovel inclination angle (X_2) are presented in Figures 10 and 11. The surface morphology and contour patterns intuitively reveal the coupling and interaction behavior of the two factors:

(1) Response surface for tuber exposure rate

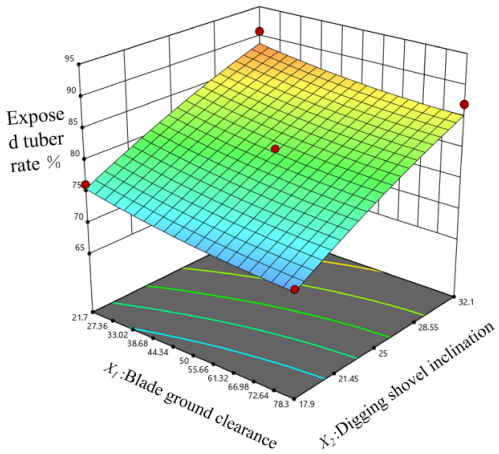

Figure 10. Response surface of tuber exposure rate.

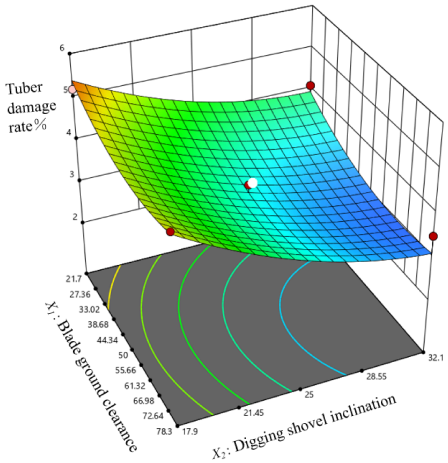

Figure 11. Response surface of tuber damage rate.

The surface shows a distinct upward trend along the axis of digging shovel inclination angle, while it exhibits only mild variation along the axis of blade-to-ridge clearance. The contour lines are approximately parallel to the X_1 axis, further confirming that digging shovel inclination angle is the dominant factor, blade-to-ridge clearance exerts a weak effect, and no significant interaction exists between the two parameters. Regardless of the level of blade-to-ridge clearance, increasing the digging shovel inclination angle consistently elevates the tuber exposure rate. When the inclination angle is fixed, adjusting blade-to-ridge clearance alone does not produce a significant improvement in the tuber exposure rate.

(2) Response surface for tuber damage rate

The surface exhibits a typical concave paraboloid shape, with its lowest point corresponding to the parameter range for minimum tuber damage ($X_1 \approx 43.7$ mm, $X_2 \approx 31.3^\circ$). At small blade-to-ridge clearance and low digging shovel inclination angle, the surface corresponds to a high-tuber-damage-rate region. As both clearance and inclination increase into the optimal range, the surface descends to the lowest-damage zone. When either parameter is increased excessively beyond the optimal range, the surface rises again and the tuber damage rate increases. This indicates that the two parameters have an optimal synergistic matching range, and deviation of a single parameter from the optimum will exacerbate tuber damage.

3.2.4. Optimization of Operating Parameters and Verification of Regression Models

Based on the dual-index regression model, a multi-objective optimization was performed using the desirability function method in Design-Expert 13 software, with the objectives of maximizing the tuber exposure rate (Y_1) and minimizing the tuber damage rate (Y_2).

Optimization settings:

Constraint range: $X_1 \in [10, 90]$ mm, $X_2 \in [15, 35]^\circ$.

Response weighting: Both Y_1 and Y_2 were assigned equal weight (weight = 1), as they are equally important for harvesting quality evaluation.

Optimization goal: maximizing the tuber exposure rate (Y_1) and minimizing the tuber damage rate (Y_2).

The global optimal parameter combination was solved as follows: blade-to-ridge clearance of 66.6 mm and digging shovel inclination angle of 34.0°, with a final overall desirability value of 0.892. Under the model-predicted optimal conditions, the tuber exposure rate and tuber damage rate were predicted to be 83.3% and 4.4%, respectively.

To verify the prediction accuracy of the regression model, five sets of replicate field validation tests were conducted using the optimal parameters. The measured average tuber exposure rate was 83.7%, and the average tuber damage rate was 4.3%. The relative errors between the measured values and the model-predicted values were 0.48% and 2.3%, respectively, which fall within the acceptable engineering tolerance range. This result confirms that the regression model has high prediction accuracy, and the optimized parameters possess good practical field applicability. Under this optimal parameter combination, the integrated machine simultaneously performs haulm shredding and tuber excavation operations.

3.2.5. Comprehensive Conclusion of Integrated Field Experiment

Digging shovel inclination angle is the core structural parameter that determines the tuber exposure rate and tuber damage rate of sweet potatoes, while blade-to-ridge clearance mainly modulates the risk of blade-induced tuber damage. Although no significant interaction effect exists between the two factors, they present an optimal synergistic matching range. From an engineering application perspective, this optimal parameter

combination also brings comprehensive benefits in power consumption and wear: the relatively large blade-to-ridge clearance reduces impact load and abrasive wear of the shredding blades, stabilizing the shredding power demand; the large shovel inclination slightly increases digging resistance but maintains it within the matching range of conventional medium-power tractors.

The existing simple grate-type separation structure achieves only preliminary tuber–soil separation, with the overall tuber exposure rate limited to 81.5–84.2%, and a small number of tubers remain buried in the soil. Future work can further optimize tuber–soil separation performance by incorporating a vibrating lifting-chain separation mechanism so as to continuously improve the tuber exposure rate index.

4. Discussion

A compact three-point hitch-mounted integrated sweet potato haulm shredding and excavating machine was developed for moist clay loam conditions in southern hilly regions of China. Two-stage field tests were performed to systematically quantify the impacts of key operating parameters on working performance. The results reveal the multi-parameter coupling mechanism of haulm shredding and harvesting quality and provide a technical basis for integrated harvesting in small hilly fields. The following section discusses the results in the context of prior research.

4.1. Pre-Harvest Haulm Shredding System Performance Mechanism

The ridge-profiled single-shaft crushing knife roller achieved a crushing qualified rate above 90%. This performance is attributed to the staggered long–short flail blade arrangement and the trochoid cutting trajectory generated by counter-rotation. Compared with the dual-shaft machine developed by Yang et al. [12], which is equipped with a front vine lifter and a secondary crushing shaft, the proposed design eliminates these additional components. By extending blade coverage to the ridge furrow, it resolves the problem of incomplete crushing at the ridge sides, resulting in a more compact, cost-effective structure better adapted to small hilly fields.

From the perspective of cutting mechanics, the counter-rotating knife roller forms a trochoid cutting trajectory, where the blade tip has a backward horizontal velocity component relative to the ground at the bottom of its path. This cutting mode avoids pushing vines forward and achieves impact–shearing composite fracture rather than simple impact crushing. The strong positive effect of knife roller speed on crushing qualified rate is consistent with this mechanism: higher rotational speed increases the relative shear velocity between the blade and the stem, improving the clean-cut rate of thick fibrous vines. At a rotational speed of 2500 r/min, the linear speed at the blade root reached 30.6 m/s, exceeding the minimum shear threshold for thick stems, validating this principle under field conditions with clay soil. Notably, blade-to-ridge clearance had no significant effect on crushing particle size, which differs from the findings of Huang et al. on potato haulm toppers [13]. This discrepancy arises because the staggered blade layout expands the vertical cutting range, compensating for variations in blade-to-ridge clearance. Nevertheless, for plots with large ridge height undulation, excessive fluctuation may cause blade–soil impact or missed cutting. A ridge-following depth-limiting mechanism is therefore recommended for future optimization.

4.2. Digging System Performance Analysis

From the perspective of soil–tool interaction, the adjustable-inclination grate-type digging shovel realizes tuber–soil separation through two sequential mechanisms: first, the inclined shovel face lifts and loosens the tuber–soil mixture, and soil clods are fractured

by normal impact and shear during sliding; second, fine soil falls through the grate bar gaps by gravity during the lifting process. Under the optimal inclination of 34.0°, the lifting height and sliding distance of the mixture reach the best balance: sufficient lifting height ensures soil fall time, while the inclination angle avoids excessive sliding acceleration that would cause tuber impact damage. The machine achieved an 83.7% tuber exposure rate and 4.3% tuber damage rate under optimal parameters. This performance satisfies harvesting requirements for hilly areas, although the tuber exposure rate is lower than that of potato harvesters equipped with forced-vibration separation chains [25], because the proposed grate structure relies only on gravity separation.

4.3. Synergistic Effect of Integrated Operation

The core challenge of integrated pre-harvest haulm shredding and excavation lies in parameter coupling and performance trade-off between the two operational units, which represents a key bottleneck restricting the widespread application of such equipment. In conventional two-stage operations, haulm shredding is performed at low blade-to-ridge clearance to achieve optimal stubble quality, with no consideration of tuber damage risk. In integrated operations, by contrast, blade-to-ridge clearance must be adjusted to balance both stubble performance and tuber safety.

Compared with the complex machine developed by Cai et al.—which adopts a disc cutter and clamping conveyor and is designed for large plain fields [14]—the machine proposed in this study combines haulm shredding with grate-type excavation. It features a more compact structure and a smaller turning radius, making it better suited for hilly fields in southern China.

In practical production, the traditional mode of "haulm shredding 2–3 days before harvesting" suffers from a long operation cycle. Autumn rainfall frequently delays harvesting and leads to tuber decay, resulting in production losses. The proposed integrated machine completes both processes in a single pass, which shortens the operation cycle and addresses the demand for timely harvest in southern China. This operation mode holds great practical value for improving mechanization levels and reducing labor costs in hilly regions.

Compared with chemical haulm killing using herbicides, the proposed mechanical shredding scheme avoids the 7–10 day waiting period for vine withering, eliminates pesticide residue risks to tubers and soil, and maintains stable performance under rainy conditions. These advantages make the integrated machine more suitable for timely harvest requirements in the autumn rainy climate of southern China. Compared with large combine harvesters, the proposed machine has a more compact structure and lower tuber damage rate, although its tuber exposure rate is relatively lower due to the simple gravity grate separation. Compared with split small machines, the proposed machine realizes single-pass integrated operation, greatly improving operational efficiency.

In terms of practical economic benefits, the proposed integrated machine reduces the field operation from two passes to one pass, improving field operation efficiency by approximately 40–50% compared with the traditional "shredding + excavation" two-stage mode. Labor demand is reduced from two to three workers per set of equipment to only one tractor operator. According to local production statistics in Guangdong, mechanized integrated harvesting can reduce harvesting cost by approximately 35–45% compared with manual harvesting, and shorten the harvesting window from 7 to 10 days to 2 to 3 days per hectare, effectively reducing the risk of tuber rot loss caused by autumn rainfall.

4.4. Limitations and Future Directions

Compared with existing large-scale integrated harvesters equipped with disc cutters, clamping conveyors and vibrating separation chains, the proposed machine adopts a simpler and more compact configuration specifically for small hilly fields.

Despite the contributions of this work, certain limitations regarding field validation remain. First, field trials were conducted only in clay loam soils (moisture content, 20–25%) typical of southern China during harvest season. For sandy soils with lower cohesion, the tuber–soil separation efficiency is expected to improve, but blade wear may accelerate; for heavy clay soils with higher moisture, soil adhesion may increase digging resistance and reduce tuber exposure rate. Second, the tested cultivar (Pushu 32) is a typical red-fleshed variety with medium tuber size; for varieties with larger tubers or shallower growth depth, the optimal blade-to-ridge clearance and shovel inclination may shift appropriately. Third, all tests were performed at a steady forward speed on flat ridge sections; operation on sloping terrain or at variable speeds may cause performance fluctuations. Second, the existing grate-type separation mechanism has limited tuber–soil separation capacity, which restricts further improvement of the tuber exposure rate. The following are recommendations for future work: (1) Integrating a lightweight vibration excitation device into the digging shovel shank to generate low-frequency, small-amplitude vibration, thereby enhancing tuber–soil separation efficiency and increasing the tuber exposure rate without a substantial rise in power consumption. (2) Conducting adaptability tests across diverse soil types, moisture levels and sweet potato cultivars to quantify the influence of environmental factors and expand the regional applicability of the machinery and parameter optimization results. (3) Developing integrated conveying and collection modules to achieve full-process mechanization covering haulm shredding, excavation and tuber collection, thereby effectively reducing the labor intensity associated with manual picking.

Overall, this study enriches the body of research on compact integrated sweet potato harvesters for hilly regions. The parameter influence patterns and optimal parameter schemes derived in this study provide a theoretical basis and technical reference for the optimization and field application of related equipment.

5. Conclusions

Addressing the challenges of separate haulm shredding and harvesting, high labor intensity, and the difficulty of mechanized harvesting in clayey soils of hilly southern China, this study designed a hitch-mounted integrated machine for sweet potato haulm shredding and tuber excavation that combines haulm shredding and returning with tuber digging. Through theoretical design, prototype fabrication, and systematic field tests, the effects of key parameters and their optimal ranges were determined. The main conclusions are as follows:

(1) The three-point hitch-mounted machine adopts a front crushing system with staggered long and short blades matching the ridge profile. The counter-rotating knife roller forms a trochoid cutting path, realizing full-coverage vine shredding on ridge surfaces and furrows. The rear grate-type digging shovel has an adjustable inclination and a width matched to the tuber distribution in high-ridge planting, enabling simultaneous lifting and gravity-based soil screening. Being compact and compatible with mainstream medium- and small-power tractors, the machine performs haulm shredding and excavation in one pass, shortening the operation cycle.

(2) Independent orthogonal field experiments on haulm shredding revealed the following: knife roller speed is a highly significant factor affecting the qualified rate of crushed stem–leaf length; forward speed is significant; and blade-to-ridge clearance has no significant effect on particle size. For stubble length, blade-to-ridge clearance is highly

significant, knife roller speed is marginally significant, and forward speed is not significant. Under the optimal parameter combination, the qualified rate of crushed stem–leaf length reached 94.4%, and stubble length fell within the agronomically acceptable range, meeting the industry standard for haulm shredding and returning.

(3) The quadratic regression models established via orthogonal rotation combination design showed satisfactory goodness of fit and non-significant lack of fit, enabling reliable prediction of harvesting performance. Digging shovel inclination had a highly significant positive effect on tuber exposure rate, whereas blade-to-ridge clearance had no significant effect. Both blade-to-ridge clearance and digging shovel inclination had significant or highly significant effects on tuber damage rate, including quadratic effects. Multi-objective optimization yielded optimal parameters of 66.6 mm blade-to-ridge clearance and 34.0° digging shovel inclination, resulting in an tuber exposure rate of 83.7% and a damage rate of 4.3%, which satisfy the requirements of NY/T 4478-2025.

(4) Field verification tests demonstrated stable performance on clay loam soil in hilly areas of southern China under the tested conditions, effectively overcoming the low efficiency and time constraints of two-stage harvesting. The machine provides a feasible technical solution for compact integrated sweet potato harvesting in hilly regions and offers reference value for improving mechanization levels in similar production areas.

Author Contributions: Conceptualization, L.H. and W.L.; methodology, L.Z., L.H. and X.G.; software, L.Z., X.G. and M.C.; validation, S.X.; formal analysis, L.Z. and K.L.; investigation, L.Z. and K.L.; resources, L.H.; data curation, L.Z., K.L. and Y.G.; writing—original draft preparation, L.Z.; writing—review and editing, K.L. and S.X.; visualization, X.G. and Y.G.; supervision, L.H. and M.C.; project administration, L.H., W.L.; funding acquisition, L.H. All authors have read and agreed to the published version of the manuscript.

Funding: This research was funded by the 2025 Guangdong Provincial Special Fund for Grain Production Safety Guarantee (Grant No. Yue Cainong [2025] No. 229), Research on Key Technologies and Equipment Development of Sweet Potato Pre-harvest Haulm Shredding Machine.

Institutional Review Board Statement: Not applicable.

Informed Consent Statement: Not applicable.

Data Availability Statement: Data are contained within the article. The data presented in this study can be requested from the authors.

Conflicts of Interest: The authors declare no conflicts of interest.

References

1. Bovell-Benjamin, A.C. Sweet potato: A review of its past, present, and future role in human nutrition. *Adv. Food Nutr. Res.* **2007**, *52*, 1–59. [CrossRef] [PubMed]
2. Food and Agriculture Organization of the United Nations. FAOSTAT Crops Database. Available online: https://www.fao.org/faostat/en/#data/QCL (accessed on 17 July 2026).
3. Li, T.; Zhou, J.; Xu, W.; Li, Q.; Zhang, H.; Qin, X.; Li, N.; Li, W.; Guo, D. Development of 4UGS2 Double-Row Sweet Potato Harvester. *Trans. Chin. Soc. Agric. Eng.* **2018**, *34*, 26–33. (In Chinese) [CrossRef]
4. Shen, H.; Wang, B.; Hu, L.; Wang, G.; Ji, L.; Shen, G.; Wu, T. Design of Sweet Potato Transfer and Conveying Mechanism for 4UZL-1 Sweet Potato Combine Harvester. *Trans. Chin. Soc. Agric. Eng.* **2020**, *36*, 9–17. (In Chinese) [CrossRef]
5. Bao, G.; Wang, G.; Hu, L.; Yang, W.; Shen, H.; Xu, X.; Wu, W.; Chen, W.; Yin, Z. Design and Optimization of Height-Adaptive Sweet Potato Collecting Device for Sweet Potato Combine Harvester. *Trans. Chin. Soc. Agric. Eng.* **2023**, *39*, 24–33. (In Chinese) [CrossRef]
6. Li, T.; Wei, X.; Jiang, W.; Li, N.; Zhang, H.; Zhou, J. Test bench study on harvesting characteristics of sweet potato vines. *Trans. Chin. Soc. Agric. Mach.* **2022**, *53*, 166–175. (In Chinese) [CrossRef]

7. Wu, T.; Hu, L.; Wang, G.; Hu, Z.; Yan, W.; Wang, B. Design and Experiment of Walking-Type Sweet Potato Vine Crushing and Returning Machine. *Trans. Chin. Soc. Agric. Eng.* **2017**, *33*, 8–17. (In Chinese) [CrossRef]
8. Chen, X.; Hu, Z.; Wang, B.; You, Z.; Peng, B.; Hu, L. Design and Parameter Optimization of Vine-Tuber Separation Mechanism for Single-Row Single-Ridge Sweet Potato Combine Harvester. *Trans. Chin. Soc. Agric. Eng.* **2019**, *35*, 12–21. (In Chinese) [CrossRef]
9. Shen, G.; Wang, G.; Hu, L.; Yuan, J.; Wang, Y.; Wu, T.; Chen, X. Development of Sweet Potato Stem Tip Harvester. *Trans. Chin. Soc. Agric. Eng.* **2019**, *35*, 46–55. (In Chinese) [CrossRef]
10. Mu, G.; Wang, W.; Zhang, T.; Hu, L.; Zheng, W.; Zhang, W. Design and Experiment with a Double-Roller Sweet Potato Vine Harvester. *Agriculture* **2022**, *12*, 1559. [CrossRef]
11. Ma, B. Research and Optimal Design of High-Clearance Sweet Potato Vine Cutting Technology and Its Device. Master's Thesis, Anhui Agricultural University, Hefei, China, 2014. (In Chinese)
12. Yang, R. Design and Experiment of Double-Shaft Sweet Potato Vine Cutting and Returning Machine. Master's Thesis, Anhui Agricultural University, Hefei, China, 2022. (In Chinese) [CrossRef]
13. Huang, X. Design of Potato Vine Killer Based on Negative Pressure Adsorption Principle. Master's Thesis, Zhongkai University of Agriculture and Engineering, Guangzhou, China, 2017. (In Chinese)
14. Cai, Y. Design and Simulation of Combined Operation Machine for Sweet Potato Harvesting and Vine Recycling. Master's Thesis, Shandong Agricultural University, Tai'an, China, 2017. (In Chinese)
15. Wu, B.; Huang, T.; Qiu, X.; Zuo, T.; Wang, X.; Xie, F. Design and Experimental Study of Potato-Soil Separation Device for Sticky Soils Condition. *Appl. Sci.* **2021**, *11*, 10959. [CrossRef]
16. Wang, G.; Peng, J.; Xue, G.; Peng, B.; Zhang, Y.; Hu, L.; Shen, H. Design of Key Components for Integrated Fresh Sweet Potato Harvesting Based on Agricultural Machinery and Agronomy: Study on Low-Damage Conveying and Separating Mechanism. *J. Agric. Food Res.* **2026**, *29*, 103043. [CrossRef]
17. Peng, J.; Wang, Y.; Peng, B.; Xue, G.; Hu, L.; Wang, G. Research Status and Prospects of Sweet Potato Harvesters' Conveying and Separation Mechanisms. *Sustainability* **2024**, *16*, 10957. [CrossRef]
18. Kakahy, A.N.N.; Ahmad, D.; Akhir, M.D.; Sulaiman, S.; Ishak, A. Effects of Knife Shapes and Cutting Speeds of a Mower on the Power Consumption for Pulverizing Sweet Potato Vine. *Key Eng. Mater.* **2013**, *594–595*, 1126–1130. [CrossRef]
19. Mu, G.; Liu, Z.; Liu, J.; Zheng, W.; Qi, X.; Wang, X.; Lü, Z. Design and Experiment on Rotary Cutting Test Bench for Sweet Potato Vine. *Am. J. Biochem. Biotechnol.* **2022**, *18*, 129–140. [CrossRef]
20. Kong, C.; Wang, Q.; Liao, Y.; Xia, J.; Jin, Y. Research and optimization of the inclination angle difference of the digging shovel surface of potato harvester in hilly areas. *Eng. Agríc.* **2025**, *45*, e20240140. [CrossRef]
21. Li, Y.Y.; Wei, N.; Pan, P.; Zheng, G.L.; Du, K.; Lü, C.W.; Luo, Q.Y.; Wang, J.C.; Tang, D.B. Effects of Mechanized Planting Density and Depth on Sweet Potato Quality Characteristics, Yield Formation and Rhizosphere Microorganisms. *Trans. Chin. Soc. Agric. Eng.* **2026**, *42*, 69–77. [CrossRef]
22. *NY/T 2706-2015*; Technical Specification for Quality Evaluation of Potato Haulm Toppers. Ministry of Agriculture of the People's Republic of China: Beijing, China, 2015. (In Chinese)
23. *JB/T 14284-2022*; Potato Haulm Toppers. Ministry of Industry and Information Technology of the People's Republic of China: Beijing, China, 2022. (In Chinese)
24. *NY/T 4478-2025*; Technical Regulations for Sweet Potato Harvesting. Ministry of Agriculture and Rural Affairs of the People's Republic of China: Beijing, China, 2025. (In Chinese)
25. Zhang, X.; Liu, J.; Zhang, C.; Zhao, Y.; Du, X. Design and Experimentation of Small Potato Harvester for Heavy Soil in Hilly and Mountainous Areas. *Agronomy* **2024**, *14*, 2131. [CrossRef]

Disclaimer/Publisher's Note: The statements, opinions and data contained in all publications are solely those of the individual author(s) and contributor(s) and not of MDPI and/or the editor(s). MDPI and/or the editor(s) disclaim responsibility for any injury to people or property resulting from any ideas, methods, instructions or products referred to in the content.